International Journal of Mechanics and Solids
ISSN 0973-1881 Volume 6, Number 1 (2011), pp. 7-26

http://www.ripublication.com/ijms.htm

On Accurate Stress Determination in Laminated Finite Length Cylinders Subjected to Thermo Elastic Load

***Payal Desai and Tarun Kant**

Department of Civil Engineering,
Indian Institute of Technology Bombay, Powai, Mumbai 400 076, India
**Corresponding Author E-mail: payaldesai79@gmail.com*

Abstract

In this paper, we analyze the boundary value problems (BVPs) of a finite length laminated cylinders under thermoelastic loads using a semi analytical cum numerical approach. Exact elasticity equations are used in the analysis without any assumptions to determine the accurate stresses. Examples covered are diaphragm supported isotropic, orthotropic and laminated composite cylinder under symmetric thermal load which is considered as a two dimensional (2D) plane strain problem of thermoelasticity in (r, z) direction. The boundary conditions are satisfied exactly by taking an analytical expression in axial (z) direction in terms of Fourier series expansion. Fundamental (basic) dependent variables are chosen in the radial coordinate of the cylinder. First order simultaneous ordinary differential equations are obtained as mathematical model which are integrated through an effective numerical integration technique by first transforming the BVP into a set of initial value problems (IVPs). The numerical results obtained are also first validated for their accuracy with 1D solution of an infinitely long cylinder.

Keywords: A. Laminate; B. Thermal properties; C. Computational mechanics; C. Deformation; C. Structural composites.

Introduction

Thermal stresses are of great practical importance, especially in large composite cylinders such as steam-turbine rotors, heavy shafts and large turbine discs. In all these cases, heating or cooling must be gradual in order to reduce the temperature gradient in the radial direction. Moreover, determination of the stresses and

deformation in thin and thick orthotropic laminated cylindrical shells subject to thermal loading is a major activity in the design of equipments such as pressure vessels, nuclear reactors, piping, boilers and heat exchangers. Composite cylinders are also widely used in various aerospace engineering applications such as aerospace vehicles, heat shields for re-entry vehicles, etc. and need accurate analysis of deformations and stresses induced by thermal loading. The classic thermal stress problem of infinitely long cylinders made of elastic isotropic materials has been studied by many long back. Kent [1] presented solutions for the stresses in solid and hollow spheres and long cylinders in which the temperature is a function of both radial coordinate and time and obtained solution by substituting in the already available formulae. Poritsky [2] gave complete 2D analytical solution related to steady-state temperature stresses in a cylindrical tube of mercury boilers where the tubes are exposed to the flame and receive radiation on one side only. Jaeger [3] gave analytical results for thermoelastic problems of infinitely long solid and hollow cylinders at constant temperature and for the case of periodic surface temperature distribution under the condition of plane stress using series of Bessel functions. Yang and Lee [4] obtained a series solution for thick- walled cylinders subjected to a temperature distribution which varied both radially and axially. The solution is based on 3D linear theory of thermoelasticity with appropriate approximations by neglecting small terms. Kalam and Tauchert [5] analysed stresses in a hollow orthotropic elastic cylinder due to a steady-state plane temperature distribution $T(r,\theta)$ using the Airy stress function. Iyengar and Chandrashekhara [6] gave a three-dimensional rigorous solution for determining thermal stresses in a finite length solid cylinder due to a steady state axisymmetric temperature field over one of its end surfaces.

In this paper, governing differential equations from exact theory of 3D thermoelasticity, which govern the behaviour of a finite length circular orthotropic/laminated cylinder in a state of plane strain in (r, z) under temperature loading which is a function of both radial and axial coordinates, are taken. By assuming a global analytical solution in the longitudinal direction which satisfies the two end boundary conditions exactly, the 2D generalized plane strain problem is reduced to a 1D problem in the radial direction. The equations are reformulated to enable application of an efficient and accurate numerical integration technique for the solution of the BVP of a cylinder. In addition, one dimensional elasticity equations of an infinitely long axisymmetric cylinder are utilized to reformulate the 1D mathematical model suitable for numerical integration. These equations are summarized in the Appendix I and II. This has been done with a view to check and compares the results of the present formulation of finite length cylinder under uniform internal/external thermal load, when the length of the cylinder tends to infinity.

Formulation

Basic governing equations of an symmetric cylinder [7] in cylindrical coordinates are (Fig.1).

Equilibrium equations

$$\frac{\partial \sigma_r}{\partial r}+\frac{\partial \tau_{zr}}{\partial z}+\frac{\sigma_r-\sigma_\theta}{r}=0$$
$$\frac{\partial \tau_{zr}}{\partial r}+\frac{\partial \sigma_z}{\partial z}+\frac{\tau_{zr}}{r}=0 \qquad (1a)$$

Strain displacement relations

$$\varepsilon_r=\frac{\partial u}{\partial r} \quad \varepsilon_\theta=\frac{u}{r} \quad \varepsilon_z=\frac{\partial w}{\partial z} \quad \gamma_{zr}=\frac{\partial w}{\partial r}+\frac{\partial u}{\partial z} \qquad (1b)$$

Stress-strains-temperature relations for cylindrically orthotropic material

$$\varepsilon_r=\frac{\sigma_r}{E_r}-\nu_{\theta r}\frac{\sigma_\theta}{E_\theta}-\nu_{zr}\frac{\sigma_z}{E_z}+\alpha_r T \quad \varepsilon_\theta=-\nu_{r\theta}\frac{\sigma_r}{E_r}+\frac{\sigma_\theta}{E_\theta}-\nu_{z\theta}\frac{\sigma_z}{E_z}+\alpha_\theta T$$
$$\varepsilon_z=-\nu_{rz}\frac{\sigma_r}{E_r}-\nu_{\theta z}\frac{\sigma_\theta}{E_\theta}+\frac{\sigma_z}{E_z}+\alpha_z T,\ \gamma_{rz}=\frac{\tau_{rz}}{G_{rz}} \qquad (1c)$$

Stresses in terms of strains can be written as follows

$$\begin{Bmatrix}\sigma_r\\ \sigma_\theta\\ \sigma_z\end{Bmatrix}=\begin{bmatrix}C_{11} & C_{12} & C_{13}\\ C_{21} & C_{22} & C_{23}\\ C_{31} & C_{32} & C_{33}\end{bmatrix}\begin{Bmatrix}\varepsilon_r-\alpha_r T\\ \varepsilon_\theta-\alpha_\theta T\\ \varepsilon_z-\alpha_z T\end{Bmatrix}$$
$$\tau_{rz}=G_{rz}\gamma_{rz} \qquad (1d)$$

where,

$$\nu_{r\theta}=\frac{\nu_{\theta r}}{E_\theta}E_r,\ \nu_{rz}=\frac{\nu_{zr}}{E_z}E_r,\ \nu_{z\theta}=\frac{\nu_{\theta z}}{E_\theta}E_z$$
$$C_{11}=\frac{E_r(1-\upsilon_{\theta z}\upsilon_{z\theta})}{\Delta},\quad C_{12}=\frac{E_r(\upsilon_{\theta r}+\upsilon_{zr}\upsilon_{\theta z})}{\Delta},\quad C_{13}=\frac{E_r(\upsilon_{zr}+\upsilon_{\theta r}\upsilon_{z\theta})}{\Delta}$$
$$C_{22}=\frac{E_\theta(1-\upsilon_{rz}\upsilon_{zr})}{\Delta},\quad C_{32}=\frac{E_\theta(\upsilon_{z\theta}+\upsilon_{r\theta}\upsilon_{zr})}{\Delta}\quad C_{33}=\frac{E_z(1-\upsilon_{r\theta}\upsilon_{\theta r})}{\Delta} \qquad (1e)$$
$$\Delta=(1-\nu_{r\theta}\nu_{\theta r}-\nu_{\theta z}\nu_{z\theta}-\nu_{zr}\nu_{rz}-2\nu_{\theta r}\nu_{z\theta}\nu_{rz})$$
$$C_{21}=C_{12},\ C_{23}=C_{32},\ C_{31}=C_{13}$$

Stresses in terms of displacement components can be cast as follows:

$$\sigma_r=C_{11}\left(\frac{\partial u}{\partial r}-\alpha_r T\right)+C_{12}\left(\frac{u}{r}-\alpha_\theta T\right)+C_{13}\left(\frac{\partial w}{\partial z}-\alpha_z T\right)$$
$$\sigma_\theta=C_{21}\left(\frac{\partial u}{\partial r}-\alpha_r T\right)+C_{22}\left(\frac{u}{r}-\alpha_\theta T\right)+C_{23}\left(\frac{\partial w}{\partial z}-\alpha_z T\right) \qquad (1f)$$

$$\sigma_z = C_{31}\left(\frac{\partial u}{\partial r} - \alpha_r T\right) + C_{32}\left(\frac{u}{r} - \alpha_\theta T\right) + C_{33}\left(\frac{\partial w}{\partial z} - \alpha_z T\right)$$

$$\tau_{rz} = G\gamma_{rz} = G\left(\frac{\partial w}{\partial r} + \frac{\partial u}{\partial z}\right)$$

and boundary conditions in the longitudinal and radial directions are,

$$at\ z = 0, l, \quad u = \sigma_z = 0;\ \ at\ r=r_i, \quad \sigma_r = \tau_{rz} = 0;\ \ at\ \ r=r_o, \quad \sigma_r = \tau_{rz} = 0 \tag{2}$$

in which l is the length, r_i is the inner radius and r_o is the outer radius of a hollow cylinder.

Radial direction r is chosen to be a preferred independent coordinate. Four fundamental dependent variables, viz., displacements, u and w and corresponding stresses, σ_r and τ_{rz} that occur naturally on a tangent plane r = constant, are chosen in the radial direction. Circumferential stress σ_θ and axial stress σ_z are treated here as auxiliary variables [8] since these are found to be dependent on the chosen fundamental variables. A set of four first order partial differential equations in independent coordinate r which involve only fundamental variables is obtained through algebraic manipulation of Eqs. (1a) and (1f). These are,

$$\frac{\partial u}{\partial r} = \frac{\sigma_r}{C_{11}} + \alpha_r T + \frac{C_{12}}{C_{11}}\left(\alpha_\theta T - \frac{u}{r}\right) + \frac{C_{13}}{C_{11}}\left(\alpha_z T - \frac{\partial w}{\partial z}\right) \tag{3a}$$

$$\frac{\partial w}{\partial r} = \frac{1}{G}\tau_{rz} - \frac{\partial u}{\partial z} \tag{3b}$$

$$\frac{\partial \sigma_r}{\partial r} = -\frac{\partial \tau_{rz}}{\partial z} + \frac{\sigma_r}{r}\left(\frac{C_{21}}{C_{11}} - 1\right) + \left(\frac{C_{21}C_{12}}{C_{11}} - c_{22}\right)\left(\frac{\alpha_\theta T}{r} - \frac{u}{r^2}\right) + \left(\frac{C_{21}C_{13}}{C_{11}} - c_{23}\right)\left(\frac{\alpha_z T}{r} - \frac{1}{r}\frac{\partial w}{\partial z}\right) \tag{3c}$$

$$\frac{\partial \tau_{rz}}{\partial r} = -\frac{\tau_{rz}}{r} - \frac{C_{31}}{C_{11}}\frac{\partial \sigma_r}{\partial z} - C_{31}\frac{\partial(\alpha_r T)}{\partial z} + \left(C_{32} - \frac{C_{12}C_{31}}{C_{11}}\right)\frac{\partial}{\partial z}\left(\alpha_\theta T - \frac{u}{r}\right) + \left(C_{33} - \frac{C_{13}C_{31}}{C_{11}}\right)\frac{\partial}{\partial z}\left(\alpha_z T - \frac{\partial w}{\partial z}\right) \tag{3d}$$

and the auxiliary variables,

$$\sigma_\theta = C_{21}\left(\frac{\partial u}{\partial r} - \alpha_r T\right) + C_{22}\left(\frac{u}{r} - \alpha_\theta T\right) + C_{23}\left(\frac{\partial w}{\partial z} - \alpha_z T\right) \tag{4a}$$

$$\sigma_z = C_{31}\left(\frac{\partial u}{\partial r} - \alpha_r T\right) + C_{32}\left(\frac{u}{r} - \alpha_\theta T\right) + C_{33}\left(\frac{\partial w}{\partial z} - \alpha_z T\right) \tag{4b}$$

A longitudinally sinusoidal/uniform and through thickness logarithmic variation of temperature is assumed as follows [14],

Type-I

$$T(r,z) = T_m \sin\frac{\pi z}{l} \quad where \quad T_m = \frac{T_0 \log\frac{r_o}{r}}{\log\frac{r_o}{r_i}} \tag{5a}$$

Type-II

$$\mathrm{T}(r,z) = T_m \sum_{i=1,3,5,\ldots}^{N} \frac{1}{i}\sin\frac{i\pi z}{l} \quad where \quad T_m = \frac{4}{\pi}\frac{\mathrm{T}_0 \log\frac{r_o}{r}}{\log\frac{r_o}{r_i}} \tag{5b}$$

A longitudinally sinusoidal/uniform and through thickness linear type variation of temperature is assumed as follows [15],

Type-III

$$\mathrm{T}(r,z) = T_m \sin\frac{\pi z}{l} \quad \text{where } T_m = \left[\mathrm{T}_1 + \frac{r}{h}T_2\right] \tag{6a}$$

Type-IV

$$\mathrm{T}(r,z) = T_m \sum_{i=1,3,5,\ldots}^{N} \frac{1}{i}\sin\frac{i\pi z}{l} \quad \text{where } T_m = \frac{4}{\pi}\left[\mathrm{T}_1 + \frac{r}{h}T_2\right] \tag{6b}$$

where T_0 is initial reference temperature, T_1 and T_2 are average and difference in rise in temperature of top and bottom surfaces of cylinder.

Variations of the four fundamental dependent variables which completely satisfy the boundary conditions of simple (diaphragm) supports at z = 0, l can then be assumed as,

$$\begin{aligned} u(r,z) &= \sum_{i=1,3,5,\ldots}^{N} U_i(r)\sin\frac{i\pi z}{l} \quad \sigma_r(r,z) = \sum_{i=1,3,5,\ldots}^{N} \sigma_i(r)\sin\frac{i\pi z}{l} \\ w(r,z) &= \sum_{i=1,3,5,\ldots}^{N} W_i(r)\cos\frac{i\pi z}{l} \quad \tau_{rz}(r,z) = \sum_{i=1,3,5,\ldots}^{N} \tau_i(r)\cos\frac{i\pi z}{l} \end{aligned} \tag{7}$$

Substitution of Eq. (7) in Eqs. (3a-d) and Eqs. (4a-b) and simplification resulting from orthogonality conditions of trigonometric functions leads to the following four simultaneous ordinary differential equations involving only fundamental variables. These are,

$$U'_i(r) = \frac{\sigma_i(r)}{C_{11}} + \alpha_r T_m + \frac{C_{12}}{C_{11}}\left(\alpha_\theta T_m - \frac{U_i(r)}{r}\right) + \frac{\mathrm{C}_{13}}{\mathrm{C}_{11}}\left(\alpha_z T_m + \frac{i\pi}{l}W_i(r)\right) \tag{8a}$$

$$W_i^{'}(r)=\frac{1}{G}\tau_{rz}(r)-U_i(r)\frac{i\pi}{l} \tag{8b}$$

$$\sigma_i^{'}(r)=\frac{i\pi}{l}\tau_{rz}(r)+\left(\frac{C_{21}}{C_{11}}-1\right)\frac{\sigma_i(r)}{r}+\left(\frac{C_{21}.C_{12}}{C_{11}}-C_{22}\right)\left(\frac{\alpha_\theta}{r}T_m-\frac{U_i(r)}{r^2}\right)+\left(\frac{C_{21}C_{13}}{C_{11}}-C_{23}\right)\left(\frac{\alpha_z}{r}T_m+\frac{i\pi}{l}\frac{W_i(r)}{r}\right) \tag{8c}$$

$$\tau_i^{'}(r)=-\frac{\tau_{rz}(r)}{r}-\frac{i\pi}{l}\frac{C_{31}}{C_{11}}\sigma_i(r)-C_{31}\left(\alpha_r\frac{i\pi}{l}T_m\right)+\left(C_{32}-\frac{C_{12}C_{31}}{C_{11}}\right)\left(\alpha_\theta\frac{i\pi}{l}T_m-\frac{i\pi}{l}\frac{U_i(r)}{r}\right)+\left(C_{33}-\frac{C_{13}C_{31}}{C_{11}}\right)\left(\alpha_z\frac{i\pi}{l}T_m+\left(\frac{i\pi}{l}\right)^2W_i(r)\right) \tag{8d}$$

and the auxiliary variables,

$$\sigma_{\theta_i}=\sum_{i=1,3,5,\ldots}^{N}\left[\frac{C_{21}}{C_{11}}\sigma_i(r)+\left(\frac{C_{21}C_{12}}{C_{11}}-C_{22}\right)\left(\alpha_\theta T_m-\frac{U_i(r)}{r}\right)+\left(\frac{C_{13}C_{21}}{C_{11}}-C_{23}\right)\left(\alpha_z T_m+\frac{i\pi}{l}W_i(r)\right)\right]\sin\frac{i\pi z}{l} \tag{9a}$$

$$\sigma_{z_i}=\sum_{i=1,3,5,\ldots}^{N}\left[\frac{C_{31}}{C_{11}}\sigma_i(r)+\left(\frac{C_{31}C_{12}}{C_{11}}-C_{32}\right)\left(\alpha_\theta T_m-\frac{U_i(r)}{r}\right)+\left(\frac{C_{13}C_{31}}{C_{11}}-C_{33}\right)\left(\alpha_z T_m+\frac{i\pi}{l}W_i(r)\right)\right]\sin\frac{i\pi z}{l} \tag{9b}$$

Solution

The above system of first order simultaneous ordinary differential equations (8a-d) together with the appropriate boundary conditions at the inner and outer edges of the cylinder (Eq (2)), forms a two-point BVP. However, a BVP in ODEs cannot be numerically integrated as only a half of the dependent variables (two) are known at the initial edge and numerical integration of an ODE is intrinsically an IVP. It becomes necessary to transform the problem into a set of IVPs. The initial values of the remaining two fundamental variables must be selected so that the complete solution satisfies the two specified conditions at the terminal boundaries during the process of integration [8]. This technique has been successfully applied and explained in detail to solutions of plate's problems [9, 10, 11, 12, and 13] in the past. However, problems related to cylindrical coordinates are uncovered in that literature. Fourth order Runge-Kutta algorithm with modifications suggested by Gill [16] is used for the numerical integration of the IVPs. A Fortran code is written for analyzing the problems.

Results and discussion

Non dimensionalized parameters are defined as follows for thermal loading, viz.,

$$\bar{r} = \frac{r}{R} \quad R = \frac{1}{2}(r_0 + r_i)$$

$$(\bar{u},\bar{w}) = \frac{1}{\alpha_r T_0 R}(u,w) \quad (\bar{\sigma}_r, \bar{\sigma}_\theta, \bar{\sigma}_z, \bar{\tau}_{rz}) = \frac{1}{\alpha_r T_0 E_r}(\sigma_r, \sigma_\theta, \sigma_z, \tau_{rz}) \tag{11}$$

A hollow cylinder is analysed by taking two h/R ratios of 1/5 and 1/50 which cover geometrically thick and thin cases. T_0 and T_2 are assumed as 1°C where as T_1 is assumed as 0 °C. Material properties for cylindrically orthotropic material are taken as follows. (Kalam and Tauchert [5])

$$E_r = 2.068\times10^7 \text{ KN/m}^2, \quad E_\theta = 20.68\times10^7 \text{ KN/m}^2, \quad E_z = 2.068\times10^7 \text{ KN/m}^2$$
$$\nu_{\theta r} = 0.25, \quad \nu_{zr} = 0.25, \quad \nu_{z\theta} = 0.025 \tag{12}$$
$$\alpha_r = 51\times10^{-6}1/°\text{C}, \quad \alpha_\theta = 8.4\times10^{-6}1/°\text{C}, \quad \alpha_z = 51\times10^{-6}1/°\text{C}$$

Radial and hoop quantities are maximum at z = *l*/2 whereas axial quantities are maximum at z = 0, *l*. Radial stresses and radial displacements, presented in Tables 1-2, for temperature variations described by Eqs. (5) and (6) for isotropic and orthotropic cylinders are compared with the plane strain elasticity solution for infinitely long cylinder, the solution given by Timoshenko and Goodier [14]. Eq. (13) shows analytical solution for radial stress, hoop stress and radial displacement from exact theory of elasticity for infinitely long cylinder under plane strain state given in Timoshenko and Goodier [14]. These are used to validate and check the present results throughout wherever applicable.

$$\sigma_r = \frac{E}{1-\upsilon}\left[-\frac{1}{r^2}\int_{r_i}^{r}\alpha T r dr + \frac{r^2 - r_i^2}{r^2(r_o^2 - r_i^2)}\int_{r_i}^{r_o}\alpha T r dr\right]$$

$$\sigma_\theta = \frac{E}{1-\upsilon}\left[\frac{1}{r^2}\int_{r_i}^{r}\alpha T r dr + \frac{r^2 + r_i^2}{r^2(r_o^2 - r_i^2)}\int_{r_i}^{r_o}\alpha T r dr - \alpha T\right] \quad u = \frac{1}{r}\frac{1+\upsilon}{1-\upsilon}\int_{r_i}^{r}\alpha T r dr + C_1 r + C_2\frac{1}{r}$$

$$\text{where, } C_1 = \frac{(1+\upsilon)(1-2\upsilon)}{1-\upsilon}\frac{1}{r_o^2 - r_i^2}\int_{r_i}^{r_o}\alpha T r dr - \upsilon\varepsilon_z, \quad C_2 = \frac{1+\upsilon}{1-\upsilon}\frac{r_i^2}{r_o^2 - r_i^2}\int_{r_i}^{r_o}\alpha T r dr \tag{13}$$

In these numerical computations, the following properties for isotropic material are used.

$$E_r = E_\theta = E_z = 2\times10^8 \text{ KN/m}^2 \quad \nu_{\theta r} = \nu_{zr} = \nu_{z\theta} = 0.3 \quad \alpha_r = \alpha_\theta = \alpha_z = 2.306\times10^{-6}1/°\text{C}$$

Three sets of numerical results are presented in tables 1-3 for clear comparison, i. e., (1) results from the present 2D finite length cylinder formulation, (2) Computations on the analytical formulae available for infinitely long cylinder under plane strain condition given in Timoshenko and Goodier [14] and (3) results from the

present 1D infinitely long cylinder for which formulation is given in Appendix which forms BVP of plane strain situation.

When the cylinder is subjected to a sinusoidal pressure load, the results within the limited central length zone only are compared with the plane strain one dimensional solutions, while in the case of an uniformly distributed load over the entire length of the cylinder, such comparisons are valid for most of the length of the cylinder except near the end supports.

A few cases out of the extensive numerical experiments carried out in the present study.

- Through thickness variations of basic dependent variables for sinusoidal temperature variation of Type-I are shown in Figs. 2 for h/R = 1/5 for finite length orthotropic cylinders of *l*/R ratios = 4 and 40.
- Figs. 3-4 shows through thickness variation of quantities for uniformly distributed thermal load of Type-II for h/R = 1/5 and in Fig. 5 for h/R=1/50.
- Fig. 6 shows through thickness variation of quantities for uniformly distributed thermal load of Type-IV for h/R = 1/5.
- Through thickness variation of basic dependent variables for sinusoidal temperature variation of Type-I are shown in Fig. 7 for h/R = 1/5 for finite length ($0^0/90^0$) layered orthotropic cylinders of *l*/R ratios = 4 and 40.
- Distribution of axial displacement $\overline{w}$ and shear stress $\overline{\tau}_{rz}$ through thickness in two layer orthotropic composite cylinder (0/90) for temperature variation Type-I and h/R=1/5 are shown in Fig. 8.
- Distribution of radial displacement $\overline{u}$ and radial stress $\overline{\sigma}_r$ through thickness in two layer orthotropic composite cylinder (0/90) for temperature variation Type-I and h/R=1/50 are shown in Fig. 9.
- Distribution of axial displacement $\overline{w}$ and shear stress $\overline{\tau}_{rz}$ through thickness in two layer orthotropic composite cylinder (0/90) for temperature variation Type-I and h/R=1/50 are shown in Fig. 10.
- Distribution of radial displacement $\overline{u}$ and radial stress $\overline{\sigma}_r$ through thickness in two layer orthotropic composite cylinder (0/90) for temperature variation Type-III and h/R=1/5 are shown in Fig. 11.
- Distribution of axial displacement $\overline{w}$ and shear stress $\overline{\tau}_{rz}$ through thickness in two layer orthotropic composite cylinder (0/90) for temperature variation Type-III and h/R=1/5 are shown in Fig. 12.
- Distribution of radial displacement $\overline{u}$ and radial stress $\overline{\sigma}_r$ through thickness in two layer orthotropic composite cylinder (0/90) for temperature variation Type-III and h/R=1/50 are shown in Fig.13.
- Distribution of axial displacement $\overline{w}$ and shear stress $\overline{\tau}_{rz}$ through thickness in two layer orthotropic composite cylinder (0/90) for temperature variation Type-III and h/R=1/50 are shown in Fig. 14.
- Distributions of radial and shear stresses are parabolic whereas radial

displacement, hoop stress and axial stress are linear through thickness. Axial displacement is constant through the thickness for all cases.

- It is seen in Tables 1-3 that for isotropic and orthotropic cylinders with *l*/R = 40, representing an infinitely long cylinder, the results are close to the plane strain analytical elasticity solution given by Timoshenko and Goodier [14].
- For uniformly distributed thermal load, a convergence study is carried out by taking different number of harmonic terms in Fourier series. A detailed convergence study is shown in Tables 4-5 for *l*/R ratios = 4, 40 and for h/R = 1/5 for temperature variation Type-II.
- From observation of the numerical results obtained in the present analysis, it was found that *l*/R ratios affect the rate of convergence. Fast convergence is obtained for *l*/R = 4 compared to *l*/R=40.
- It can be seen from Table 3 that for an isotropic cylinder of h/R=1/5, radial displacement converges at N = 23 for *l*/R = 4, and N = 40 for *l*/R = 40; axial displacement at N = 27 for *l*/R = 4 and N = 65 for *l*/R = 40.
- It can further be seen from Table 6 that for an orthotropic cylinder of h/R = 1/5, radial displacement converges at N = 19, axial displacement at N = 27 for *l*/R = 4. Poor convergence is seen for shear and radial stresses in both the cases. Results presented here are for harmonics N = 103 terms both for *l*/R = 4 and *l*/R = 40.

Table 1: Non-dimensional radial stress $\overline{\sigma}_r$ (z=*l*/2) and radial displacement $\overline{u}$ (z=*l*/2) through thickness for diaphragm supported elastic isotropic cylinder under temperature variation Type-I for υ=0.3 and h/R=1/5.

Present-Finite length cylinder $\overline{\sigma}_r$ (z=*l*/2)						Present infinitely long cylinder and [14]	Present-Finite length cylinder $\overline{u}$ (z=*l*/2)					Present infinitely long cylinder and [14]
$\overline{r}$			*l*/R						*l*/R			
	1	4	10	50	200		1	4	10	50	200	
0.9	0.0000	0.0000	0.0000	0.0000	0.0000	0.0000	0.1279	0.4044	0.4176	0.4199	0.4200	0.4200
0.92	-0.0209	-0.0151	-0.0148	-0.0147	-0.0147	-0.0147	0.1577	0.4316	0.4445	0.4468	0.4469	0.4469
0.94	-0.0342	-0.0259	-0.0253	-0.0252	-0.0252	-0.0252	0.1828	0.4544	0.4671	0.4693	0.4694	0.4694
0.96	-0.0411	-0.0327	-0.0320	-0.0319	-0.0319	-0.0319	0.2035	0.4730	0.4855	0.4877	0.4878	0.4878
0.98	-0.0428	-0.0359	-0.0354	-0.0353	-0.0353	-0.0353	0.2199	0.4876	0.5000	0.5021	0.5022	0.5022
1	-0.0405	-0.0361	-0.0356	-0.0355	-0.0355	-0.0355	0.2323	0.4983	0.5106	0.5127	0.5128	0.5128
1.02	-0.0350	-0.0334	-0.0330	-0.0330	-0.0330	-0.0330	0.2408	0.5053	0.5175	0.5196	0.5197	0.5197
1.04	-0.0273	-0.0281	-0.0280	-0.0279	-0.0279	-0.0279	0.2456	0.5087	0.5209	0.5230	0.5231	0.5231
1.06	-0.0184	-0.0207	-0.0206	-0.0206	-0.0206	-0.0206	0.2466	0.5086	0.5208	0.5230	0.5230	0.5231
1.08	-0.0090	-0.0112	-0.0112	-0.0112	-0.0112	-0.0112	0.2441	0.5052	0.5175	0.5197	0.5197	0.5198
1.1	0.0000	0.0000	0.0000	0.0000	0.0000	0.0000	0.2379	0.4987	0.5110	0.5132	0.5133	0.5133

Table 2: Comparison of non-dimensional radial displacement $\bar{u}$ (z=*l*/2) and radial stress $\overline{\sigma_r}$ (z=*l*/2) through thickness for diaphragm supported elastic *isotropic* cylinder under thermal loading of Type-I and II and for h/R=1/5 with elasticity plane strain solution for infinitely long cylinder and finite cylinder from the present work.

	Present - Finite length cylinder $\bar{u}$ *(z=l/2)*				Present infinitely long cylinder and [14]	Present- Finite length cylinder $\overline{\sigma_r}$ *(z=l/2)*				Present infinitely long cylinder and [14]
	Sinusoidal temperature (i)		Uniformly distributed temperature (ii)			Sinusoidal temperature (i)		Uniformly distributed temperature (ii)		
$\overline{r}$	*l*/R=4	*l*/R=40	*l*/R=4	*l*/R=40		*l*/R=4	*l*/R=40	*l*/R=4	*l*/R=40	
0.9	0.4044	0.4199	0.4239	0.4192	0.4200	0.0000	0.0000	0.0000	0.0000	0.0000
0.92	0.4316	0.4468	0.4499	0.4463	0.4469	-0.0151	-0.0147	-0.0136	-0.0149	-0.0147
0.94	0.4544	0.4693	0.4716	0.4691	0.4694	-0.0259	-0.0252	-0.0231	-0.0255	-0.0252
0.96	0.4730	0.4877	0.4892	0.4877	0.4878	-0.0327	-0.0319	-0.0290	-0.0323	-0.0319
0.98	0.4876	0.5021	0.5029	0.5023	0.5022	-0.0359	-0.0353	-0.0320	-0.0356	-0.0353
1	0.4983	0.5127	0.5130	0.5129	0.5128	-0.0361	-0.0355	-0.0324	-0.0359	-0.0355
1.02	0.5053	0.5196	0.5195	0.5199	0.5197	-0.0334	-0.0330	-0.0303	-0.0333	-0.0330
1.04	0.5087	0.5230	0.5226	0.5233	0.5231	-0.0281	-0.0279	-0.0260	-0.0281	-0.0279
1.06	0.5086	0.5230	0.5224	0.5233	0.5231	-0.0207	-0.0206	-0.0195	-0.0207	-0.0206
1.08	0.5052	0.5197	0.5191	0.5201	0.5198	-0.0112	-0.0112	-0.0109	-0.0113	-0.0112
1.1	0.4987	0.5132	0.5127	0.5136	0.5133	0.0000	0.0000	0.0000	0.0000	0.0000

Table 3: Comparison of non-dimensional radial displacement $\bar{u}$ (z=*l*/2) and radial stress $\overline{\sigma_r}$ (z=*l*/2) through thickness for diaphragm supported elastic *orthotropic* cylinder under thermal loading of Type-I and II and for h/R=1/5 with elasticity plane strain solution for infinitely long cylinder and finite cylinder from the present work.

	Present $\bar{u}$ *(z=l/2)*				Present infinitely long cylinder	Present $\overline{\sigma_r}$ *(z=l/2)*				Present infinitely long cylinder
	Sinusoidal temperature (i)		Uniformly distributed temperature (ii)			Sinusoidal temperature (i)		Uniformly distributed temperature (ii)		
$\overline{r}$	*l*/R=4	*l*/R=40	*l*/R=4	*l*/R=40		*l*/R=4	*l*/R=40	*l*/R=4	*l*/R=40	
0.9	0.0149	0.0160	0.0162	0.0164	0.0198	0.0000	0.0000	0.0000	0.0000	0.0000
0.92	0.0368	0.0379	0.0379	0.0381	0.0392	-0.0304	-0.0302	-0.0277	-0.0299	-0.0270
0.94	0.0551	0.0562	0.0563	0.0564	0.0558	-0.0506	-0.0504	-0.0458	-0.0499	-0.0452
0.96	0.0703	0.0714	0.0715	0.0715	0.0698	-0.0624	-0.0621	-0.0567	-0.0616	-0.0559
0.98	0.0826	0.0837	0.0837	0.0837	0.0814	-0.0670	-0.0668	-0.0615	-0.0663	-0.0603
1	0.0921	0.0932	0.0932	0.0931	0.0908	-0.0656	-0.0655	-0.0609	-0.0650	-0.0594
1.02	0.0990	0.1001	0.1002	0.1000	0.0981	-0.0592	-0.0592	-0.0555	-0.0589	-0.0539
1.04	0.1035	0.1046	0.1047	0.1045	0.1035	-0.0488	-0.0489	-0.0461	-0.0486	-0.0446
1.06	0.1057	0.1068	0.1069	0.1067	0.1070	-0.0350	-0.0351	-0.0334	-0.0350	-0.0322
1.08	0.1058	0.1068	0.1074	0.1067	0.1088	-0.0186	-0.0187	-0.0180	-0.0186	-0.0172
1.1	0.1037	0.1048	0.1082	0.1046	0.1090	0.0000	0.0000	0.0000	0.0000	0.0000

Table 4: Values of non-dimensional basic dependent variables at r = R for diaphragm supported finite length isotropic cylinder of ratio *h*/R = 1/5 under uniformly distributed loading for temperature variation Type-II-a convergence study for *l*/R ratios = 4, 40.

		l/R = 4				*l*/R = 40		
N	$\sum\overline{u}$	$\sum\overline{w}$	$\sum\overline{\sigma_r}$	$\sum\overline{\tau_{rz}}$	$\sum\overline{u}$	$\sum\overline{w}$	$\sum\overline{\sigma_r}$	$\sum\overline{\tau_{rz}}$
1	0.634779	-0.762446	-0.045924	0.036925	0.653079	-7.573287	-0.045230	0.003552
5	0.513703	-0.708326	-0.039506	0.032069	0.565568	-7.034692	-0.039224	0.003575
11	0.513877	-0.692628	-0.032892	0.011750	0.487164	-6.910668	-0.033608	-0.000101
13	0.511101	-0.698092	-0.038183	0.019666	0.534952	-6.955767	-0.037186	0.003684
15	0.513010	-0.694016	-0.032372	0.013588	0.494276	-6.921943	-0.034063	-0.000171
19	0.512576	-0.694709	-0.031461	0.014334	0.498786	-6.927147	-0.034324	-0.000248
21	0.511969	-0.696704	-0.039939	0.018023	0.525585	-6.944493	-0.036622	0.003836
25	0.512142	-0.696444	-0.040915	0.017808	0.522810	-6.942758	-0.036470	0.003905
29	0.512142	-0.696271	-0.041696	0.017715	0.520555	-6.941023	-0.036362	0.003957
33	0.512229	-0.696184	-0.042238	0.017671	0.518820	-6.940156	-0.036275	0.003979
37	0.512229	-0.696184	-0.042541	0.017647	0.517346	-6.939289	-0.036210	0.003964
41	0.512229	-0.696097	-0.042650	0.017619	0.516219	-6.939289	-0.036145	0.003912
49	0.512229	-0.696010	-0.042498	0.017541	0.514571	-6.938421	-0.036036	0.003712
53	0.512229	-0.696010	-0.042303	0.017487	0.514050	-6.938421	-0.035993	0.003584
57	0.512229	-0.695924	-0.042086	0.017422	0.513617	-6.937554	-0.035971	0.003448
61	0.512229	-0.695924	-0.041826	0.017359	0.513356	-6.937554	-0.035928	0.003311
65	0.512229	-0.695924	-0.041565	0.017296	0.513096	-6.937554	-0.035906	0.003179
69	0.512229	-0.695924	-0.041305	0.017242	0.513010	-6.937554	-0.035885	0.003055
73	0.512229	-0.695924	-0.041045	0.017173	0.512923	-6.937554	-0.035863	0.002942
77	0.512229	-0.695924	-0.040785	0.017142	0.512836	-6.937554	-0.035841	0.002838
79	0.512229	-0.695663	-0.030160	0.015497	0.513270	-6.935820	-0.035212	0.000758
83	0.512229	-0.695663	-0.030356	0.015564	0.513270	-6.935820	-0.035234	0.000846
87	0.512229	-0.695663	-0.030616	0.015588	0.513270	-6.935820	-0.035234	0.000924
91	0.512229	-0.695663	-0.030703	0.015705	0.513270	-6.935820	-0.035256	0.000994
95	0.512229	-0.695663	-0.030919	0.015724	0.513270	-6.935820	-0.035256	0.001056
99	0.512229	-0.695663	-0.031223	0.015620	0.513270	-6.935820	-0.035256	0.001112

Table 5: Values of non-dimensional basic dependent variables at r = R for diaphragm supported finite length orthotropic cylinder of ratio *h*/R = 1/5 under uniformly distributed loading for temperature variation Type-II-a convergence study for *l*/R ratios = 4, 40.

		l/R=4				*l*/R=40		
N	$\sum\overline{u}$	$\sum\overline{w}$	$\sum\overline{\sigma_r}$	$\sum\overline{\tau_{rz}}$	$\sum\overline{u}$	$\sum\overline{w}$	$\sum\overline{\sigma_r}$	$\sum\overline{\tau_{rz}}$
1	0.117333	-0.772941	-0.083537	0.026717	0.118706	-7.729411	-0.083404	0.002662
5	0.098667	-0.718039	-0.072691	0.026509	0.102863	-7.180391	-0.072283	0.002664
9	0.094157	-0.711765	-0.070264	0.022460	0.099059	-7.117646	-0.069638	0.002667
13	0.093294	-0.709804	-0.069524	0.018782	0.097373	-7.101960	-0.068481	0.002672

19	0.093294	-0.707059	-0.061323	0.010306	0.090431	-7.070587	-0.063409	-0.000017
27	0.093216	-0.707451	-0.060508	0.011463	0.091333	-7.078430	-0.063997	-0.000029
31	0.093216	-0.707843	-0.060204	0.011709	0.091608	-7.078430	-0.064177	-0.000033
35	0.093216	-0.707843	-0.060034	0.011861	0.091843	-7.078430	-0.064319	-0.000036
39	0.093216	-0.707843	-0.059977	0.011965	0.092039	-7.078430	-0.064433	-0.000036
41	0.093294	-0.708235	-0.071013	0.014477	0.094353	-7.082352	-0.066528	0.002698
45	0.093255	-0.708235	-0.070927	0.014402	0.094196	-7.082352	-0.066443	0.002693
49	0.093255	-0.708235	-0.070795	0.014335	0.094078	-7.082352	-0.066376	0.002684
53	0.093255	-0.708235	-0.070624	0.014269	0.093961	-7.082352	-0.066310	0.002671
57	0.093255	-0.708235	-0.070434	0.014193	0.093843	-7.082352	-0.066263	0.002653
61	0.093255	-0.708235	-0.070226	0.014136	0.093765	-7.082352	-0.066215	0.002629
67	0.093216	-0.707843	-0.061058	0.012449	0.092824	-7.082352	-0.064841	0.000076
69	0.093255	-0.708235	-0.069847	0.014003	0.093647	-7.082352	-0.066149	0.002570
73	0.093255	-0.708235	-0.069647	0.013956	0.093569	-7.082352	-0.066111	0.002534
77	0.093255	-0.708235	-0.069439	0.013937	0.093529	-7.082352	-0.066092	0.002495
81	0.093255	-0.708235	-0.069259	0.013899	0.093490	-7.082352	-0.066064	0.002455
89	0.093255	-0.708235	-0.068917	0.013842	0.093412	-7.082352	-0.066026	0.002367
93	0.093255	-0.708235	-0.068775	0.013814	0.093373	-7.082352	-0.066007	0.002323
95	0.093216	-0.707843	-0.062224	0.012742	0.093137	-7.082352	-0.065011	0.000362
97	0.093255	-0.708235	-0.068832	0.013624	0.093333	-7.082352	-0.065988	0.002278
99	0.093216	-0.707843	-0.062328	0.012809	0.093137	-7.082352	-0.065021	0.000407

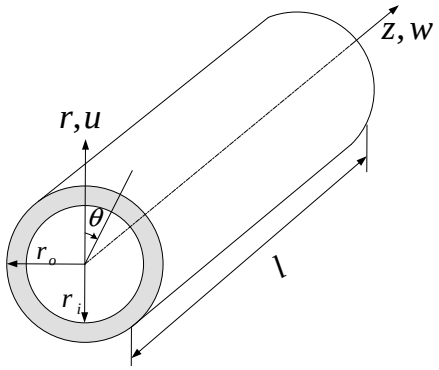

Figure 1a: Coordinate system and geometry of cylinder.

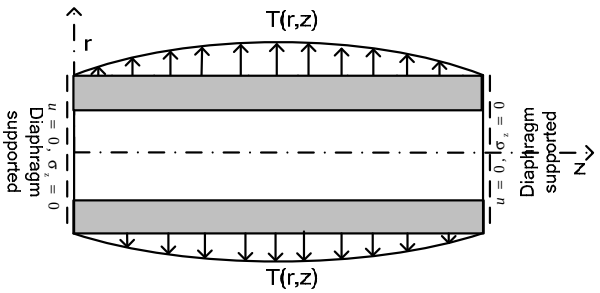

Figure 1b: Finite cylinder under sinusoidal external thermal loading.

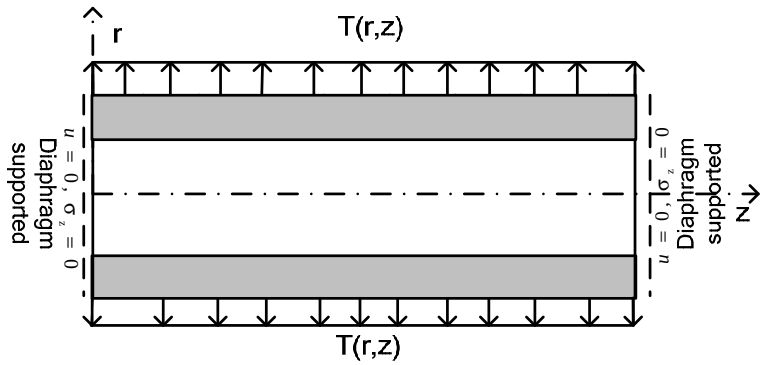

Figure 1c: Finite cylinder under uniformly distributed external thermal loading.

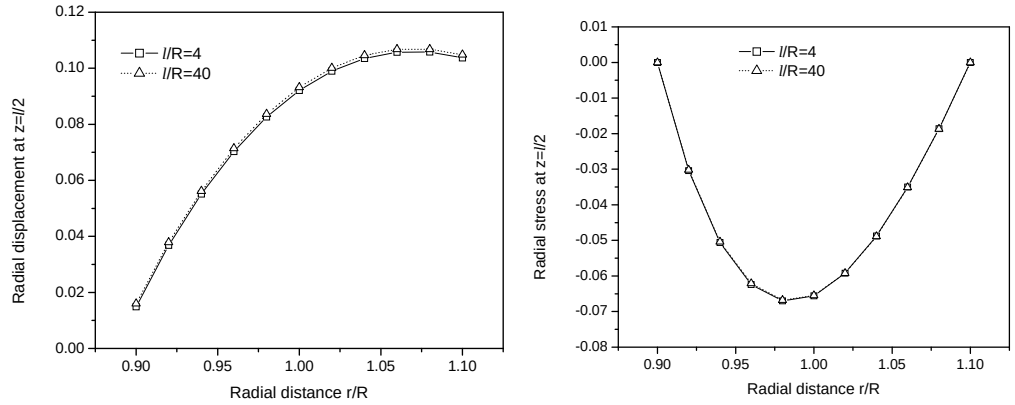

Figure 2: Distribution of radial displacement $\bar{u}$ and radial stress $\overline{\sigma_r}$ through thickness in orthotropic cylinder for temperature variation Type-I and h/R=1/5.

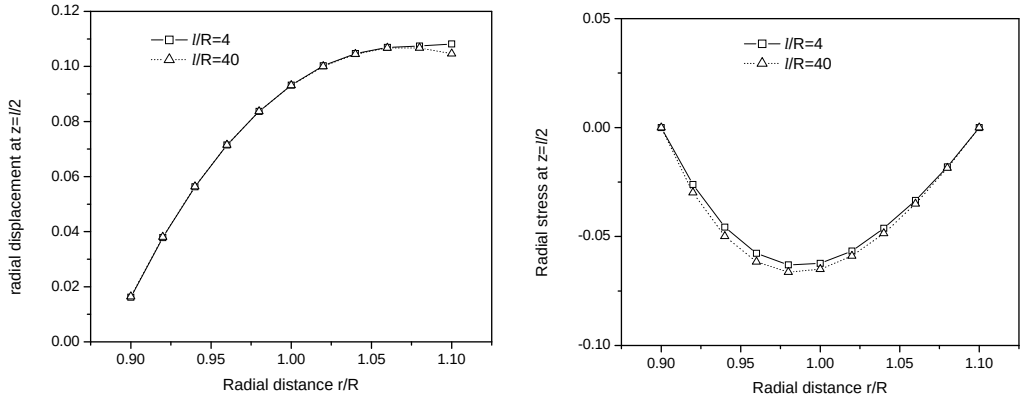

Figure 3: Distribution of radial displacement $\bar{u}$ and radial stress $\overline{\sigma_r}$ through thickness in orthotropic cylinder for temperature variation Type-II and h/R=1/5.

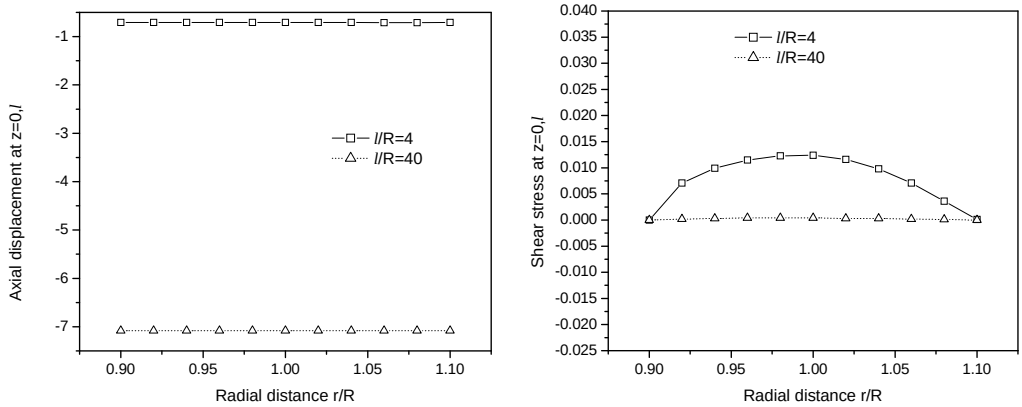

Figure 4: Distribution of axial displacement $\overline{w}$ and shear stress $\overline{\tau_{rz}}$ through thickness in orthotropic cylinder for temperature variation Type-II and h/R=1/5.

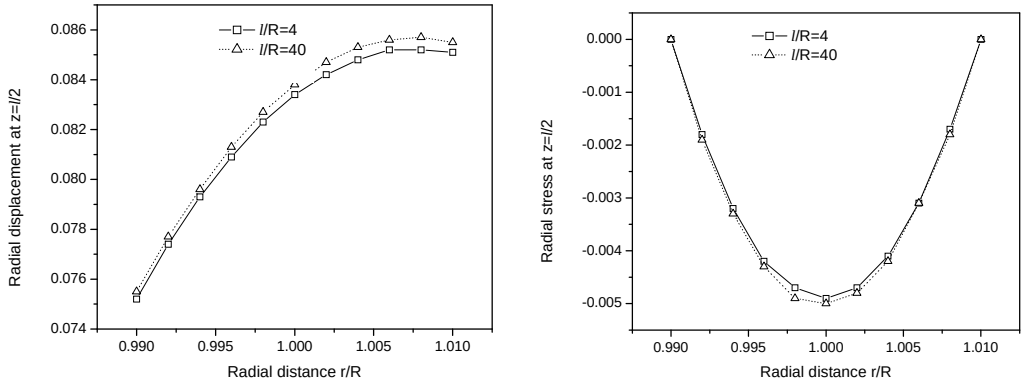

Figure 5: Distribution of radial displacement $\overline{u}$ and radial stress $\overline{\sigma_r}$ through thickness in orthotropic cylinder for temperature variation Type-II and h/R=1/50.

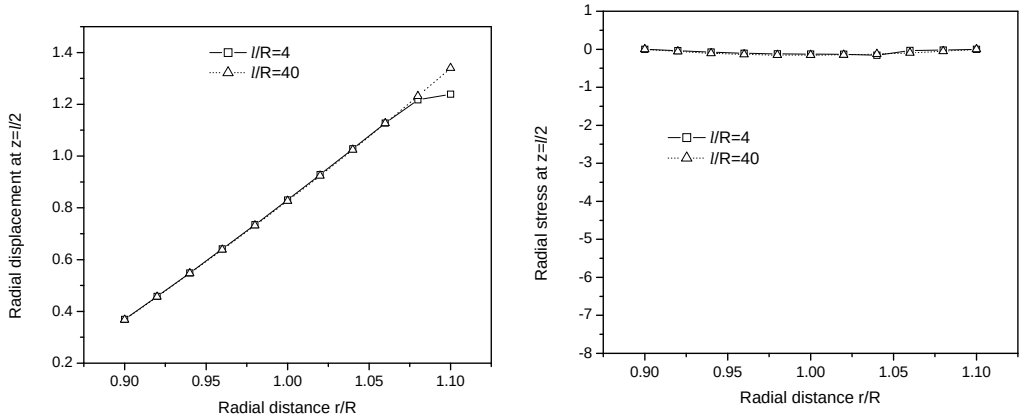

Figure 6: Distribution of radial displacement $\overline{u}$ and radial stress $\overline{\sigma_r}$ through thickness in orthotropic cylinder for temperature variation Type-IV and h/R=1/5.

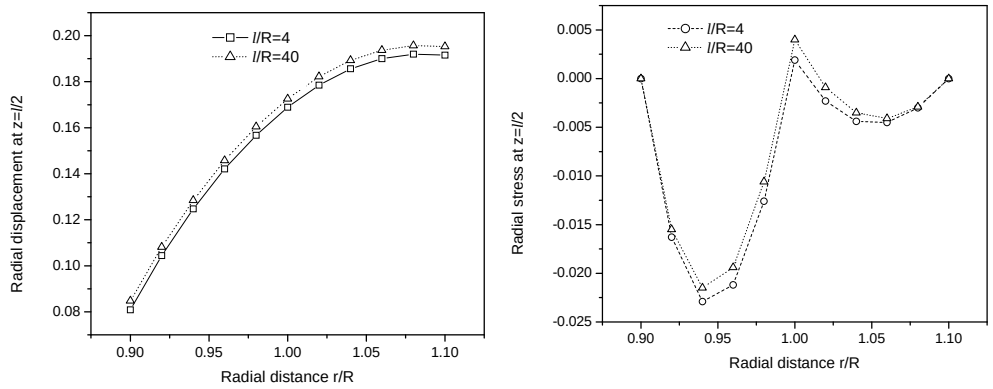

Figure 7: Distribution of radial displacement $\bar{u}$ and radial stress $\overline{\sigma_r}$ through thickness in two layer orthotropic composite cylinder (0/90) for temperature variation Type-I and h/R=1/5.

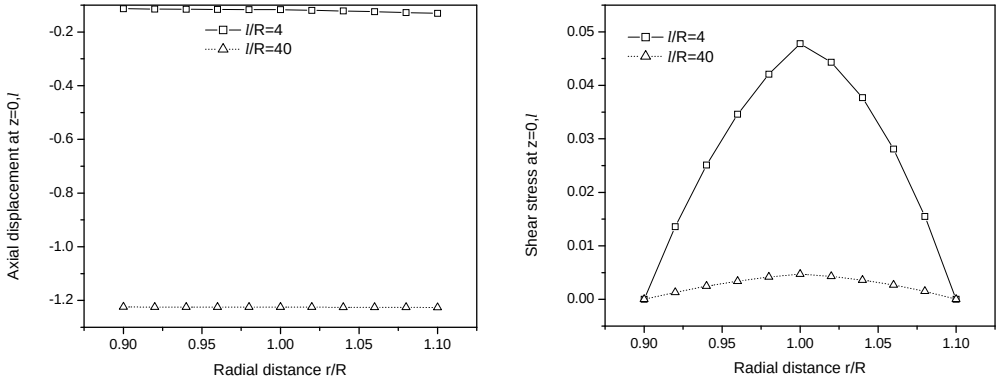

Figure 8: Distribution of axial displacement $\overline{w}$ and shear stress $\overline{\tau_{rz}}$ through thickness in two layer orthotropic composite cylinder (0/90) for temperature variation Type-I and h/R=1/5.

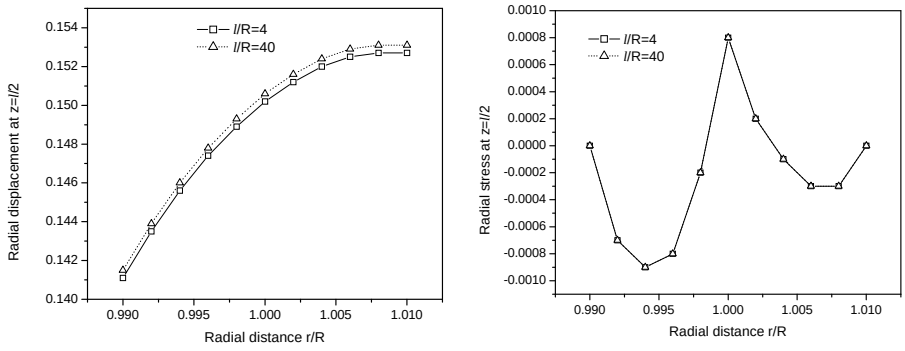

Figure 9: Distribution of radial displacement $\bar{u}$ and radial stress $\overline{\sigma_r}$ through thickness in two layer orthotropic composite cylinder (0/90) for temperature variation Type-I and h/R=1/50.

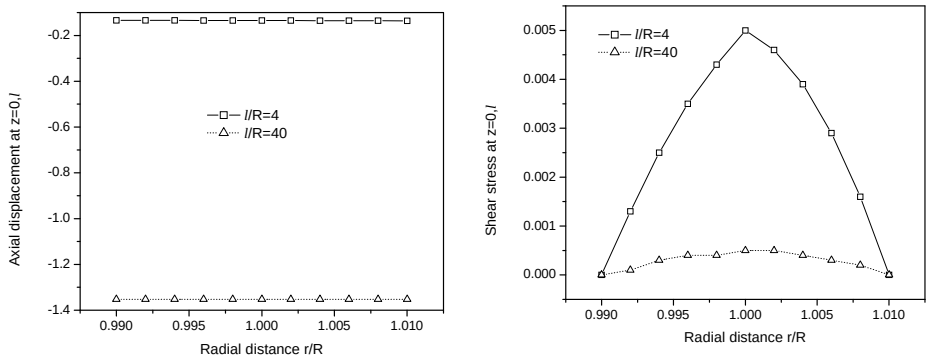

Figure 10: Distribution of axial displacement $\overline{w}$ and shear stress $\overline{\tau_{rz}}$ through thickness in two layer orthotropic composite cylinder (0/90) for temperature variation Type-I and h/R=1/50.

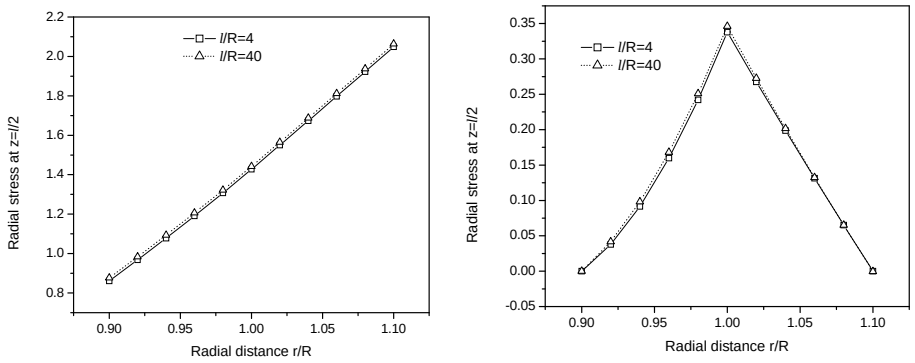

Figure 11: Distribution of radial displacement $\overline{u}$ and radial stress $\overline{\sigma_r}$ through thickness in two layer orthotropic composite cylinder (0/90) for temperature variation Type-III and h/R=1/5.

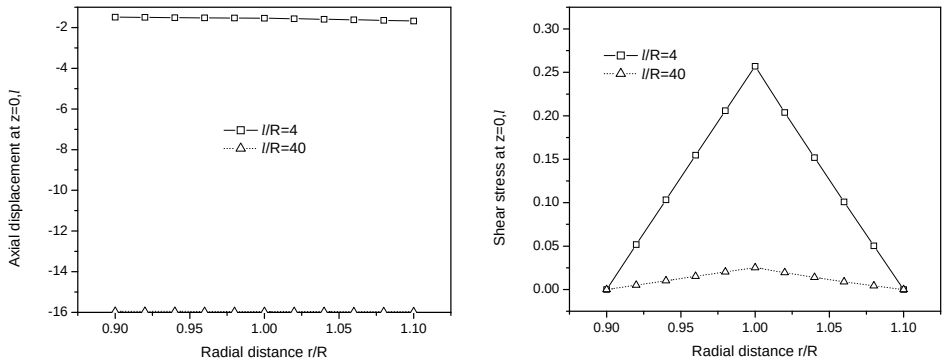

Figure 12: Distribution of axial displacement $\overline{w}$ and shear stress $\overline{\tau_{rz}}$ through thickness in two layer orthotropic composite cylinder (0/90) for temperature variation Type-III and h/R=1/5.

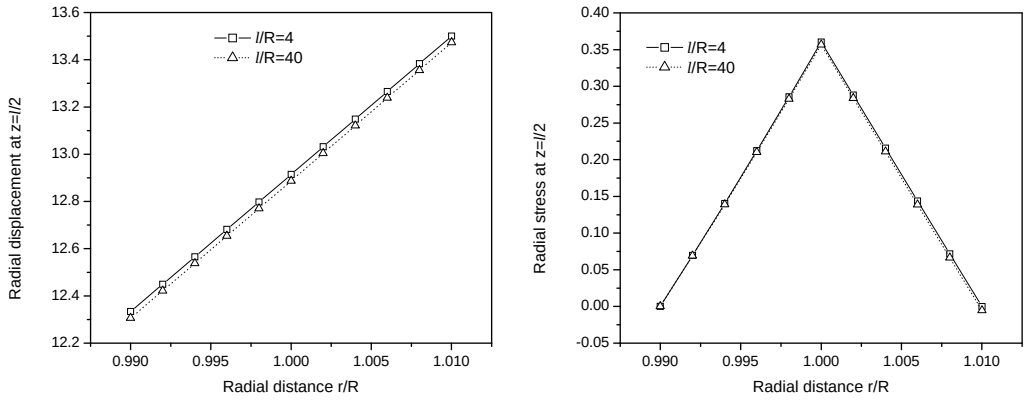

Figure 13: Distribution of radial displacement $\bar{u}$ and radial stress $\overline{\sigma_r}$ through thickness in two layer orthotropic composite cylinder (0/90) for temperature variation Type-III and h/R=1/50.

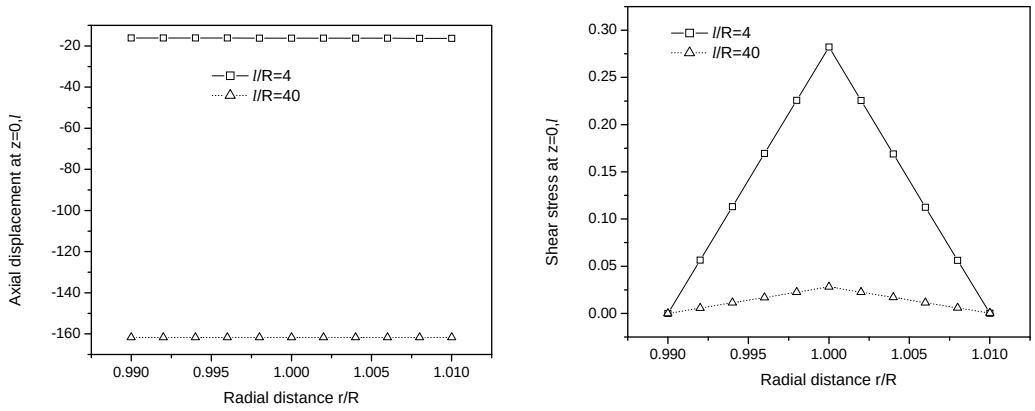

Figure 14: Distribution of axial displacement $\bar{w}$ and shear stress $\overline{\tau_{rz}}$ through thickness in two layer orthotropic composite cylinder (0/90) for temperature variation Type-III and h/R=1/50.

Conclusions

Numerical analysis of elastic isotropic, orthotropic and laminated fiber reinforced composite cylinders under sinusoidal and uniformly distributed thermal loadings of two types are presented. Mathematical model is based on the exact theory of elasticity without any kinematic and kinetic assumptions. Basic equations are cast in a form suitable for numerical integration in the radial direction. Numerical integration technique adopted here is found to be very effective and accurate; as (1) it incorporates mixed variables both stresses and displacements in the analysis (2) continuity conditions through thickness for layered materials are directly satisfied while performing the integration.

Acknowledgements

Partial support of a USIF collaborative project grant IND104 is gratefully acknowledged.

Nomenclature

r, θ, z	Cylindrical coordinates
u,v,w	Displacement components
σ_r , σ_θ , σ_z	Normal stress components parallel to r, θ, and z axis
τ_{zr}	Shearing stress in cylindrical coordinates
ε_r , ε_θ , ε_z , γ_{zr}	Unit elongations (normal and shear strain) components in cylindrical coordinates
E	Young's modulus of elasticity
α	Coefficient of thermal expansion per degree centigrade
T	Temperature rise at any point in a cylinder
ν	Poisson's ratio
r_i , r_0	Inner and outer radius of the cylinder
l	Length of the cylinder
T_0 ,T_1,T_2	Initial reference temperature
p	Uniform external pressure
$\bar{u}, \bar{w}$	Nondimensionalized displacement components
$\bar{\sigma}_r, \bar{\sigma}_\theta, \bar{\sigma}_z$,	Nondimensionalized normal stress components parallel to r, θ, and z axis
$\bar{\tau}_{rz}$	Nondimensionalized shearing stress in cylindrical coordinates
$\bar{r}$	Nondimensionalized radius
R	Mean radius $\frac{(r_0 + r_i)}{2}$

References

[1] Kent, C. H., 1932, "Thermal Stresses in Spheres and Cylinders," ASME J. of Appl. Mech., 54, 185-196.

[2] Poritsky, H., 1937, "Thermal Stresses in Cylindrical Pipes," Phil.Mag. S., 7(24), 160, 209-222.

[3] Jaeger, J. C. 1945, "On Thermal Stresses in Circular Cylinders," Phil. Mag., 36: 418-428.

[4] Yang, K.W., Lee CW., 1971 "Thermal Stresses in Thick-Walled Circular Cylinders under Axisymmetric Temperature Distribution," ASME J. of Engg Industry., 93(B), 969-75.

[5] Kalam, M.A., Tauchert TR. 1978, "Stresses in orthotropic elastic cylinder due to a plane temperature distribution T(r,θ)," J. of Therm. Stress; 1, 13-24.
[6] Sundara Raja Iyenger, K.T., Chandrashekhara K. 1966, "Thermal Stresses in a finite solid cylinder due to an axisymmetric temperature field at the end surface," Nucl. Engg. Design; 3, 21-31.
[7] Boley, B.A., Weiner J.H., 1960, "Theory of Thermal Stresses," New York, Wiley.
[8] Kant, T., Ramesh, C.K., 1981, "Numerical Integration of Linear Boundary Value Problems in Solid Mechanics by Segmentation Method," Int J Num Meth. in Engg, 17, 1233-1256.
[9] Kant, T., Setlur, A.V. 1973, "Computer analysis of clamped-clamped and clamped supported cylindrical shells," J. Aero. Soc. of India; 25, 47-55.
[10] Ramesh, CK, Kant T, Jadhav VB. 1974, "Elastic analysis of cylindrical pressure vessels with various end closures," Int. J. of Press. Vess. and Pip., 2, 143-154.
[11] Kant, T. 1981, "Numerical analysis of elastic plates with two opposite simply supported ends by segmentation method," Comp. and Struct., 14, 195-203.
[12] Kant, T. 1982, "Numerical analysis of thick plates," Comp. Meth. Appl. Mech. and Engg., 31, 1-18.
[13] Kant, T, Hinton E. 1983, "Mindlin plate analysis by segmentation method," ASCE J. Engg. Mech., 109, 537-556.
[14] Timoshenko, S., Goodier J.N., 1951, "Theory of Elasticity," New York, McGraw-Hill.
[15] Khare, R.K., Kant, T., Garg, A.K. 2003, "Closed-form Thermo-mechanical Solutions of Higher-order Theories of Cross-ply Laminated Shallow Shells," Comp. Struct., 59, 313-340.
[16] Gill, S., 1951, "A process for the step-by-step integration of differential equations in an automatic digital computing machine," Proc. Camb. Phil. Soc., 47(1), 96-108.

Appendix I

1d and 2d Formulation for isotropic cylinder under thermal loading

$$\frac{\partial \sigma_r}{\partial r} + \frac{\sigma_r - \sigma_\theta}{r} = 0$$

$$\varepsilon_r = \frac{\partial u}{\partial r} \qquad \varepsilon_\theta = \frac{u}{r} \tag{A1}$$

$$\sigma_r = \frac{E}{(1+\upsilon)(1-2\upsilon)}\left[(1-\upsilon)\varepsilon_r + \upsilon\varepsilon_\theta\right] - \frac{\alpha T E}{1-2\upsilon}\,,\ \sigma_\theta = \frac{E}{(1+\upsilon)(1-2\upsilon)}\left[(1-\upsilon)\varepsilon_\theta + \upsilon\varepsilon_r\right] - \frac{\alpha T E}{1-2\upsilon}$$

$$\frac{du}{dr}=\frac{\sigma_r}{\lambda(1-\upsilon)}-\frac{\upsilon}{1-\upsilon}\frac{u}{r}+\frac{\alpha TE}{\lambda(1-\upsilon)(1-2\upsilon)}$$
$$\frac{d\sigma_r}{dr}=\frac{\sigma_r}{r}\left(\frac{\upsilon}{1-\upsilon}-1\right)+\frac{u}{r^2}\left(\frac{\lambda(1-2\upsilon)}{(1-\upsilon)}\right)+\frac{\alpha TE}{r(1-2\upsilon)}\left(\frac{\upsilon}{1-\upsilon}-1\right) \quad \text{(A2)}$$

2D formulation for isotropic cylinder under thermal loading is,

$$\frac{\partial u}{\partial r}=\frac{1}{(1-\nu)}\sigma_r-\frac{\nu}{1-\nu}\frac{u}{r}-\frac{\nu}{(1-\nu)}\frac{\partial w}{\partial z}+\frac{\alpha ET}{\lambda(1-\nu)(1-2\nu)},\ \frac{\partial w}{\partial r}=\frac{1}{G}\tau_{rz}-\frac{\partial u}{\partial z}$$
$$\frac{\partial \sigma_r}{\partial r}=-\frac{\partial \tau_{rz}}{\partial z}-\frac{\sigma_r}{r}+\lambda\frac{u}{r^2}\frac{(1-2\nu)}{(1-\upsilon)}+\frac{\sigma_r}{r}\frac{\upsilon}{1-\upsilon}+\frac{\lambda}{r}\frac{\partial w}{\partial z}\frac{\upsilon(1-2\upsilon)}{(1-\upsilon)}-\frac{\alpha ET}{(1-\upsilon)} \quad \text{(A3)}$$
$$\frac{\partial \tau_{rz}}{\partial r}=-\frac{1}{r}\tau_{rz}-\frac{\lambda(1-2\upsilon)}{(1-\upsilon)}\frac{\partial^2 w}{\partial z^2}-\frac{\nu}{1-\nu}\frac{\partial \sigma_r}{\partial z}-\frac{\nu\lambda(1-2\nu)}{1-\nu}\frac{\partial}{\partial z}\left(\frac{u}{r}\right)-\alpha E\frac{(2\upsilon-1)}{(1-\upsilon)(1-2\upsilon)}\frac{\partial}{\partial z}\{T\}$$

where $\lambda=\frac{E}{(1+\nu)(1-2\nu)}$ *and* $G=\frac{E}{2(1+\nu)}$

Appendix II

1d Formulation for orthotropic cylinder under thermal loading

$$\frac{d\sigma_r}{dr}+\frac{1}{r}(\sigma_r-\sigma_\theta)=0\ ,\ \varepsilon_r=\frac{\partial u}{\partial r}\qquad \varepsilon_\theta=\frac{u}{r} \quad \text{(A4)}$$
$$\sigma_r=C_{11}(\varepsilon_r-\alpha_r T)+C_{12}(\varepsilon_\theta-\alpha_\theta T)\quad \sigma_\theta=C_{12}(\varepsilon_r-\alpha_r T)+C_{22}(\varepsilon_\theta-\alpha_\theta T)$$
$$\sigma_r=C_{11}\frac{du}{dr}-C_{11}\alpha_r T+C_{12}\frac{u}{r}-C_{12}\alpha_\theta T\quad \sigma_\theta=C_{21}\frac{du}{dr}-C_{21}\alpha_r T+C_{22}\frac{u}{r}-C_{22}\alpha_\theta T$$
$$\frac{du}{dr}=\frac{\sigma_r}{C_{11}}+\alpha_r T-\frac{C_{12}}{C_{11}}\frac{u}{r}+\frac{C_{12}}{C_{11}}\alpha_\theta T,$$
$$\frac{d\sigma_r}{dr}=\frac{\sigma_r}{r}\left(\frac{C_{21}}{C_{11}}-1\right)+\frac{u}{r^2}\left(C_{22}-\frac{C_{21}C_{12}}{C_{11}}\right)+\frac{\alpha_\theta T}{r}\left(\frac{C_{21}C_{12}}{C_{11}}-C_{22}\right) \quad \text{(A5)}$$

Where,

$$\nu_{r\theta}=\frac{\nu_{\theta r}}{E_\theta}E_r,\ C_{11}=\frac{E_r}{(1-\upsilon_{r\theta}\upsilon_{\theta r})},\quad C_{12}=\frac{\upsilon_{r\theta}E_\theta}{(1-\upsilon_{r\theta}\upsilon_{\theta r})},\ C_{22}=\frac{E_\theta}{(1-\upsilon_{r\theta}\upsilon_{\theta r})},\quad C_{21}=C_{12}$$